Eur. Phys. J. B **36**, 391–399 (2003)
DOI: 10.1140/epjb/e2003-00358-1

THE EUROPEAN PHYSICAL JOURNAL B

Percolation of polyatomic species on a square lattice

V. Cornette, A.J. Ramirez-Pastor, and F. Nieto[a]

Departamento de Física, Universidad Nacional de San Luis, CONICET, Chacabuco 917, 5700 San Luis, Argentina

Received 15 May 2003 / Received in final form 3 September 2003
Published online 23 December 2003 –

Abstract. In this paper, the percolation of (a) linear segments of size k and(b) k-mers of different structures and forms deposited on a square lattice have been studied. In the latter case, site and bond percolation have been examined. The analysis of results obtained by using finite size scaling theory is performed in order to test the universality of the problem by determining the numerical values of the critical exponents of the phase transition occurring in the system. It is also determined that the percolation threshold exhibits a exponentially decreasing function when it is plotted as a function of the k-mer size. The characteristic parameters of that function are dependent not only on the form and structure of the k-mers but also on the properties of the lattice where they are deposited.

PACS. 64.60.Ak Renormalization-group, fractal, and percolation studies of phase transitions – 68.35.Rh Phase transitions and critical phenomena – 68.35.Fx Diffusion; interface formation

1 Introduction

The study of random percolation have been attracting a great deal of interest for many years and the activity in this field is still growing [1–8]. Some aspects of the percolation process like the geometrical phase transitions occurring in the system have gained a particular impetus due to the introduction of techniques like Monte Carlo (MC) simulations and series expansions [7,9]. Despite of the number of contributions to this problem, there are many aspects which are not yet completely solved. In fact, most of the studies are devoted to the percolation of molecules with single occupancy. However, if some sort of correlation exists, like particles occupying several (k) contiguous lattice sites (k-mers), the statistical problem (multisite statistics) becomes exceedingly difficult.

The difficulty in the analysis of multisite statistics is mainly associated to three factors which differentiate the k-mers statistics from the usual single particle statistics, namely:

i) No statistical equivalence exists between particles and vacancies.
ii) The occupation of a given lattice site ensures that at least one of its nearest-neighbor sites is also occupied.
iii) An isolated vacancy cannot serve for determining whether or not that site can ever become occupied.

For these reasons, it has been difficult to formulate, in an analytical way, the statistics (and kinetics) of occupation for correlated particles. However, several attempts were done in the past in order to solve the k-mers equilibrium problem. An early seminal contribution to dimer statistics was done by Fowler and Rushbrooke [10] while an isomorphous system, namely adsorption of binary liquid in two dimensions, was treated by Flory [11,12]. The thermodynamic of dimers was made for partially [13,14] and full coverage lattice [15,16] using exact and approximate methods. More recently, Monte Carlo simulation techniques have largely contributed to the understanding of the basis of the problem [17–20].

The deposition (or irreversible adsorption) of particles on solid surfaces is a subject of considerable practical importance. In fact, in many experiments on adhesion of colloidal particles and proteins on solid substrates, the relaxation time scales are much longer than the times of the formation of the deposit. As a consequence, the study of irreversible adsorption of k-mers has also received considerable attention in the last years. A well known example of an irreversible monolayer deposition process is the random sequential adsorption (RSA). This process is well described in the literature and has been investigated extensively in the last decades [21–24]. The analysis of such phenomenon includes theoretical studies, Monte Carlo simulations and experimental results. Exact solutions are possible, mostly for one-dimensional problems [25].

From a different point of view, several authors have produced seminal contributions for analyzing the percolation of polyatomic species on different lattices [25–31]. More recently, in references [32–34] the percolation behavior of a RSA of linear segments with different size and the percolation of dissociative dimers have been studied,

[a] e-mail: fnieto@unsl.edu.ar

respectively. In both cases, the dependencies of the percolation threshold with the parameters of the problem and the universality of the phase transition present in the system has been discussed. However, the formers are limited due to finite size effects while the later is just restricted to the case $k = 2$. In this context, the present paper deals with the percolation of k-mers on a square lattice in the framework of a MC analysis. A detailed study of the finite size effects is presented in order to discuss the universality class of the phase transition which the system undergoes. The main aim of the paper is to determine the dependence of the percolation threshold on both the size and form of the percolating k-mers and the properties of the lattice where they are deposited.

The paper is organized as follows. In Section 2 the basis of the model of deposition of k-mers on either sites or bonds of a square lattice is presented. The analysis of results obtained by using finite size scaling theory is discussed in Section 3. The main purpose of this section is to test the universality of the problem by determining the numerical values of the critical exponents of the phase transition. In Section 4 we discuss the dependence of the percolation threshold on parameters of interest of the model. Finally, conclusions are drawn in Section 5.

2 The model

Let us consider a periodic square lattice of linear size L on which k-mers are deposited at random. Three different situations have been considered. In the first (second) of them, a k-uple of nearest neighbor sites (bonds) is randomly selected; if it is vacant, the k-mer is then adsorbed on those sites (bonds). Otherwise, the attempt is rejected. In any case, the procedure is iterated until N k-mers are adsorbed and the desired concentration [given by $p = (kN)/L^2$ $(p = (kN)/(2L)^2)$] is reached. In addition, the case when linear k-uples of sites (aligned along one of the lattice axes) are dropped onto the lattice has also been investigated.

The central idea of the percolation theory is based in finding the minimum concentration p for which a cluster [a group of occupied sites (bonds) in such a way that each site (bond) has at least one occupied nearest neighbor site (bond)] extends from one side to the opposite one of the system. This particular value of the concentration rate is named *critical concentration* or *percolation threshold* and determines a phase transition in the system. In the random percolation model, a single site (or a bond connecting two sites) is occupied with probability p. For the precise value of p_c, the percolation threshold of sites (bonds), at least one spanning cluster connects the borders of the system [indeed, there exist a finite probability of finding n (> 1) spanning clusters [35–38]]. In that case, a second order phase transition appears at p_c which is characterized by well defined critical exponents.

As it was already mentioned, the main goal of this paper is (a) to determine how the percolation threshold is modified whether the size of the k-mer increases and (b) to verify the universality class of the phase transition involved in the problem. For these purposes, long scale numerical simulations (independent of the size of the k-mer) are required in order to predict the behavior of the system in the thermodynamic limit. The ratio k/L is kept constant for avoiding spurious effects due to the k-mer size in comparison with the lattice size. A study of the finite-size effects allows us to make a reliable extrapolation to the $k \to \infty$ limit when the limit $L \to \infty$ is taken before. Details of this study will be given below.

3 Finite-size scaling

It is well known that it is a quite difficult matter to analytically determine, the value of the percolation threshold for a given lattice [2,4,5,7,8]. For some special types of lattices, geometrical considerations enable to derive their percolation thresholds exactly. Thus, exact thresholds are known for (a) square, triangular and honeycomb lattices and (b) triangular and Kagomm'e lattice concerning to the bond and site problem, respectively. In both cases, analytical results are obtained when a monomeric species is considered. For different conditions, i.e. for systems which do not present such a topological advantage, percolation thresholds have to be estimated numerically by means of computer simulations. An illustrative example is the percolation of polyatomic species which adds a new ingredient to the problem: the influence of local correlation.

As the scaling theory predicts [9], the larger the system size to study, the more accurate the values of the threshold obtained therefrom. Thus, the finite-size scaling theory give us the basis to achieve the percolation threshold and the critical exponents of a system with a reasonable accuracy. For this purpose, the probability $R = R_L^X(p)$ that a lattice composed of $L \times L$ elements (sites or bonds) percolates at concentration p can be defined [2]. Here, as in references [39,40], the following definitions can be given according to the meaning of X: a) $R_L^{R(D)}(p) =$ the probability of finding a rightward (downward) percolating cluster; b) $R_L^I(p) =$ the probability that we find a cluster which percolates both in a rightward and in a downward direction; c) $R_L^U(p) =$ the probability of finding either a rightward or a downward percolating cluster and d) $R_L^A(p) \equiv \frac{1}{2}\left[R_L^R(p) + R_L^D(p)\right] \equiv \frac{1}{2}\left[R_L^I(p) + R_L^U(p)\right]$.

The first step for determining the percolation threshold consists in evaluating the effective threshold $p_c(L)$ for a lattice of finite size L. In the MC simulations, $R_L^X(p)$ is determined for each discrete value of p according to the considered regular finite lattice. In order to express $R_L^X(p)$ as a function of continuous values of p, it is convenient to fit $R_L^X(p)$ to some approximation function through the least mean-square method. The fitting curve is carried out using the error function because $dR_L^X(p)/dp$ is expected to behave like the Gaussian distribution [2,39,40]:

$$\frac{dR_L^X(p)}{dp} = \frac{1}{\sqrt{2\pi}\Delta_L^X} \exp\left[-\frac{1}{2}\left[\frac{p - p_c^X(L)}{\Delta_L^X}\right]^2\right] \quad (1)$$

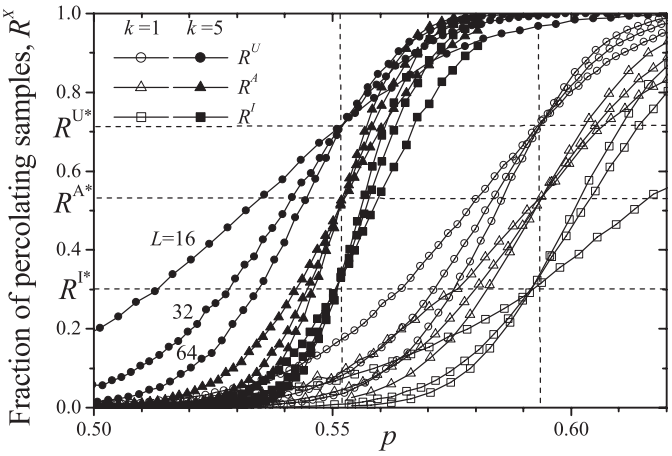

Fig. 1. Fraction of percolating lattices as a function of the concentration p defined as $p = kN/L^2$ where k is the k-mer size, N the number of deposited k-mers and L the lattice size. Different criteria are used for establishing the spanning cluster, namely, $R_L^U(p)$ the probability of finding either a rightward or a downward percolating cluster (circles); $R_L^I(p)$ the probability that we find a cluster which percolates both in a rightward and in a downward direction (squares); $R_L^A(p) \equiv \frac{1}{2}\left[R_L^R(p) + R_L^D(p)\right] \equiv \frac{1}{2}\left[R_L^I(p) + R_L^U(p)\right]$ (triangles). Open symbols represent curves for $k = 1$ while filled symbols denote the case $k = 5$. Horizontal dashed lines show the R^{X^*} universal points. Vertical dashed lines denote the percolation threshold in the thermodynamic limit $L \to \infty$.

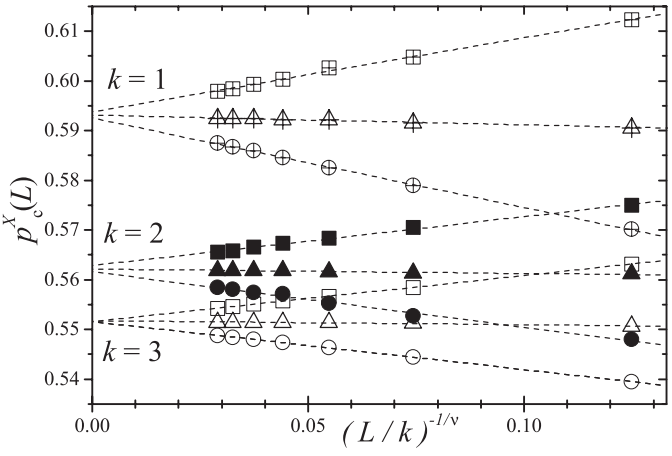

Fig. 2. Extrapolation of $p_c(k)$ towards the thermodynamic limit according to the theoretical prediction given by equation (3). Squares, triangles and circles denote the values of $p_c(k)$ obtained by using the criteria I, A and U, respectively. Different values of k are presented as indicated.

where $p_c^X(L)$ is the concentration at which the slope of $R_L^X(p)$ is the largest and Δ_L^X is the standard deviation from $p_c^X(L)$.

These considerations allow us to establish a strategy for determining the percolation threshold. Thus, each MC run consists of the following steps: (a) the construction of the lattice for a given coverage and (b) the cluster analysis by using the Hoshen and Kopelman algorithm [41]. In the late step, the number of clusters, n_s, of size s (a cluster of size s is composed by s connected elements) is determined in order to verify whether exists a percolating island. This spanning cluster could be determined by using the criteria R, D, I or U. n runs of such two steps are carried out for obtaining the number m^X of them for which a percolating cluster of the desired criterion X is found. Then, $R_L^X(p) = m^X/n$ is defined and the procedure is repeated for different both values of p and lattice sizes. A set of $n = 5\times10^4$ independent samples are numerically prepared for each value of p and L ($L/k = 16, 32, 48, 64, 80, 96, 112$).

In Figure 1, the probabilities $R_L^I(p)$ (squares), $R_L^U(p)$ (circles) and $R_L^A(p)$ (triangles) are presented for the problem of site percolation. Two different values of k are shown, open (filled) symbols represent $k = 1$ ($k = 5$). From a first inspection of the figure (and from data do not shown here for a sake of clarity) it is observed that: (a) curves cross each other in a unique universal point, R^{X^*}, which depends on the criterion X used; (b) those points do not modify their numerical value for the different k-sizes used (ranged between $k = 1$ to $k = 25$) as an indication that the universality class of the phase transition involved in the problem is conserved no matter the value of k; (c) those points are located at very well defined values in the p-axes determining the critical percolation threshold for each k and (d) p_c shifts to the left upon increasing the k-mer size. These observations are a clear indication of that (i) the percolation threshold decreases upon increasing k and (ii) the problem belongs to the same universality class no matter the size k used in the experiment.

Taking into account equation (1), for each curve $R_L^X(p)$, $p_c^X(L)$, Δ_L^X and $(\frac{dR_L^X(p)}{dp})_{max}$ are determined by least mean-square fitting. The second step is the extrapolation of $p_c^X(L)$ toward the limit $L \to \infty$ by using the scaling hypothesis. Thus, the correlation length, ξ, can be expressed as:

$$\xi \propto |p - p_c|^{-\nu} \tag{2}$$

where ν is the critical exponent which is analytically shown to be equal to $\nu = 4/3$ in the case of random percolation. As $p = p_c^X(L)$ the correlation length reaches to the linear dimension L of the lattice. Thus, we have

$$p_c^X(L) = p_c(\infty) + A^X L^{-1/\nu} \tag{3}$$

where A^X is a non-universal constant. Figure 2 shows the extrapolation towards the thermodynamic limit of $p_c^X(L)$ according to equation (3) for different values of k as indicated. This figure lends support to the assertion given by equation (3): (a) all the curves (different criteria) are well correlated by a linear function, (b) they have a quite similar value for the ordinate in the limit $L \to \infty$ and (c) the fitting determines a different value of the constant A depending of the type of criterion used. It is also important to note that $p_c^A(L)$ gives a perfect horizontal line which is a great advantage of the method because it does not require precise values of critical exponents in the process of estimating percolation thresholds. The maximum of the differences between $|p_c^I(\infty) - p_c^A(\infty)|$ and $|p_c^U(\infty) - p_c^A(\infty)|$ give the error bar for each determination of p_c.

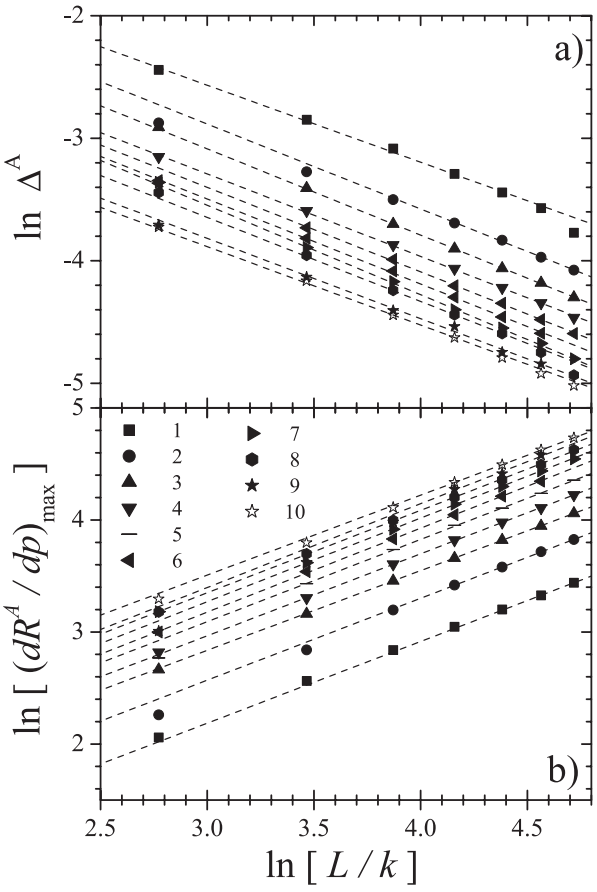

Fig. 3. a) $\ln\left(\Delta_L^A\right)$ as a function of $\ln(L/k)$ for different k-mers as indicated. According to equation (4) the slope of each line corresponds to $-1/\nu$. b) $\ln\left(\frac{dR}{dp}\right)_{max}$ as a function of $\ln(L/k)$ for different values of k. The symbols have the same meaning as in (a). According to equation (7) the slope of each line correspond to $1/\nu$.

As it was mentioned, (i) the correlation length ξ at this point is similar to L, and (ii) taking into account equation (3), we can write equation (2) in the following form:

$$\Delta_L^X \propto L^{-1/\nu}. \tag{4}$$

As an example of the validity of the last equation, Figure 3a shows Δ_L^A as a function of L/k (note the log-log scale) for different k-mers as indicated. According to equation (4), the slope of each line corresponds to $-1/\nu$. The values obtained for this critical exponent are plotted (stars) as a function of k in Figure 4.

Another alternative way for evaluating ν is given through the scaling relationship for R^X

$$R^X = \overline{R^X}\left((p-p_c)\,L^{1/\nu}\right), \tag{5}$$

being $\overline{R^X}(u)$ the scaling function.

The derivative of this expression is:

$$\frac{dR^X}{dp} = L^{1/\nu}\overline{R^X}\left((p-p_c)\,L^{1/\nu}\right) \tag{6}$$

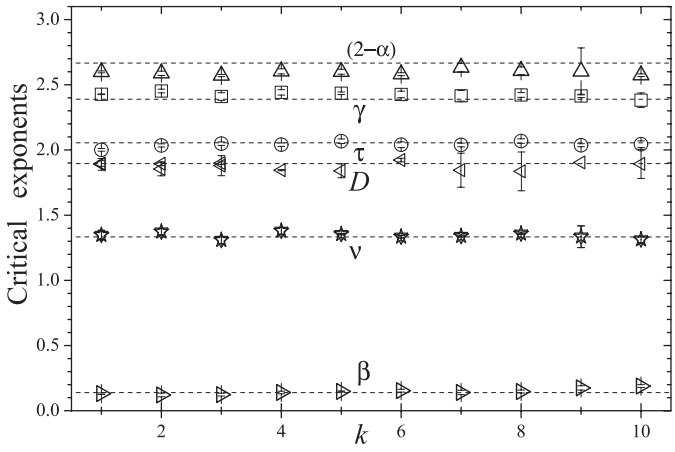

Fig. 4. Critical exponents, α, β, γ, ν, τ and the fractal dimension of the spanning cluster, D as a function of k.

which leads to

$$\left(\frac{dR^X}{dp}\right)_{max} \propto L^{1/\nu}. \tag{7}$$

In Figure 3b we have plotted $\left(\frac{dR^A}{dp}\right)_{max}$ as a function of L/k (note the log-log scale) for different k-mers as indicated. According to equation (7) the slope of each line corresponds to $1/\nu$. The values obtained for ν using this procedure are plotted (down triangles) as a function of k in Figure 4. As is clearly seen from this analysis, the problem belongs to the same universality class that the random percolation regardless of the value of k considered.

The scaling law hypothesis also predicts the collapsing of the curves $R_L^X(p)$ when they are plotted as a function of a reduced variable $u = (p-p_c)\,L^{1/\nu}$, see equation (5). Thus, $\overline{R^X}$ is a universal function with respect to the variable u. In Figure 5a, we plot R^A as a function of u for each value of k as indicated (each value of k is represented by using a different symbol). Similar behavior can be obtained for U and I criteria. Two main conclusions can be drawn from the figure. Namely, a) for a given value of k, all the curves used in the experiment (for different values of L/k) collapse into an universal curve according to the theoretical prediction. This gives an additional proof for the numerical value of the critical exponent ν. b) $\overline{R^X}$ is not only a function of p and L but also of k. As it can be seen, the collapsing function is different for each value of k considered. This fact determines that the scaling function $\overline{R^X}$ is not an universal function with respect to the variable k.

In order to determine the dependence of $\overline{R^X}$ with k, the main features of the data shown in Figure 5a have to be considered. As it can be seen, the curves become more steeper upon increasing the value of k. In fact, the derivatives of the universal function $\overline{R^X}$ with respect to u behave as a Gaussian-like function. Thus, we can observe that:

a) the derivatives become more pronounced as k increases. It is possible to establish a power law

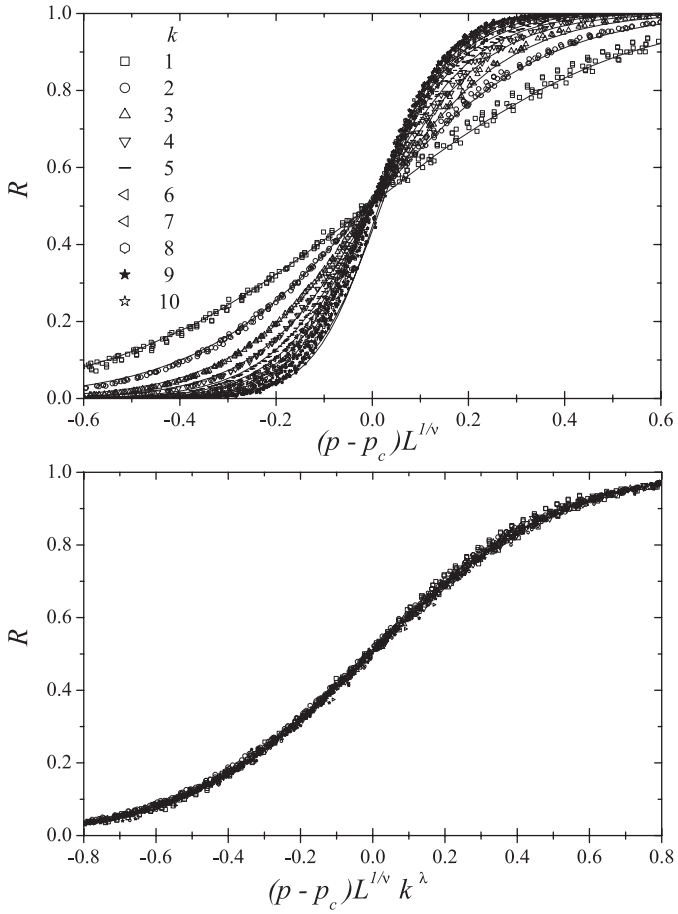

Fig. 5. a) Collapsing plot of the curves for the fraction of percolating samples as a function of u. Each symbol denotes a different value of k as indicated. For each k, all the studied lattice sizes ($L/k = 16, 32, 48, 64, 80, 96$ and 112) have been considered. The solid lines are simply a guide for the eye. b) The probability R as a function of the argument $u' = (p - p_c)\, L^{1/\nu} k^{\lambda}$ where the metric factor k^{λ} is included in order to collapse all the curves in Figure 5a onto a single one.

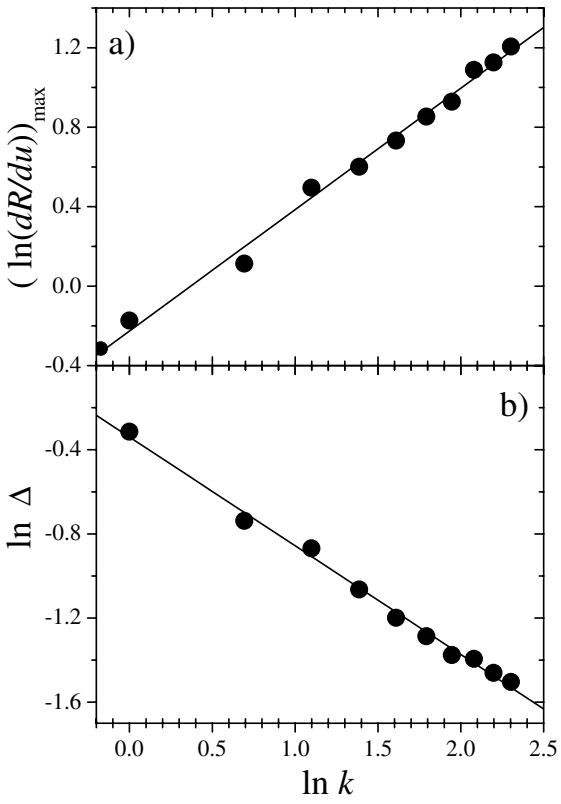

Fig. 6. a) The maxima of the derivatives of $\overline{R}$ for each value of k as a function of the k-mer size in a log-log scale. b) The standard deviation of each derivative ($\frac{\partial R}{\partial u}$) for different values of k as a function of the k-mer size (log-log scale). In both cases the lines are least mean-square fitting.

to describe this behavior. Then,

$$\left(\frac{\partial R^X}{\partial u}\right)_{max} = Bk^{\theta}. \tag{8}$$

In Figure 6a, the maxima of the derivatives for each value of k as a function of k are plotted in a log-log scale. The points are very well correlated by a linear function, equation (8), being the fitting parameters $B = 0.79 \pm 0.01$ and $\theta = 0.61 \pm 0.01$ for the three criteria used here.

b) The derivatives are narrowed upon increasing k. This behavior can also be described by a power law according to:

$$\Delta^X = Ck^{-\lambda}. \tag{9}$$

where Δ^X is the standard deviation of $\left(\frac{\partial R^X}{\partial u}\right)$ for each curve. In Figure 6b, the standard deviation of each derivative versus k is plotted in a log-log scale. The points are very well correlated by a linear function, equation (9), being the fitting parameters $C = 0.71 \pm 0.01$ and $\lambda = 0.55 \pm 0.01$ for A, U and I criteria.

According to the equations above, a metric factor might to be included in the scaling function, equation (5) in order to collapse all the curves in Figure 5a onto a single one. Following reference [42], in Figure 5b we plot the probability R^X as a function of the argument $u' = (p - p_c)\, L^{1/\nu} k^{\lambda}$. As it is clearly observed, all the curves in Figure 5a collapse onto a single one. It is remarkable that more than 6×10^3 points are included in the collapsing curve. The metric factor introduced here, k^{λ}, gives an additional proof for the numerical value of the exponent λ obtained in equation (9).

In the MC simulations, the cluster number distribution n_s can be easily obtained. The m-moments of this distribution allow us a complete determination of the associated critical exponents. In fact, according to the scaling theory applied to the percolation problem, for p close to p_c,

$$M_o = \sum n_s(p) \propto (p - p_c)^{2-\alpha} \tag{10}$$

$$M_1 = P = \sum s n_s(p) \propto (p - p_c)^{\beta} \tag{11}$$

$$M_2 = S = \sum s^2 n_s(p) \propto (p - p_c)^{-\gamma}. \tag{12}$$

Following to Stauffer [2], taking into account equation (2) and noticing that the correlation length, ξ, at the critical threshold is about L,

$$M_o \propto L^{-\frac{2-\alpha}{\nu}} \tag{13}$$

$$M_1 \propto L^{-\frac{\beta}{\nu}} \tag{14}$$

$$M_2 \propto L^{\frac{\gamma}{\nu}}. \tag{15}$$

When these relations are illustrated in a log-log scale, the slope of the corresponding lines are, respectively, $\frac{2-\alpha}{\nu}$, $\frac{\beta}{\nu}$ and $\frac{\gamma}{\nu}$ from which α, β and γ can be obtained (ν has been already determined for any of the equivalent strategies given by either Eq. (4) or Eq. (7)).

As an illustrative example, in Figure 7a we have plotted the average cluster size, S, (second moment of the n_s distribution) as a function of the rate L/k for different values of k as indicated. For each k, (a) the points are very well linearly correlated and (b) from the slope, the critical exponent γ can be determined. The lines obtained are parallel as a clear indication of that the universality of the problem remains being the same no matter the value of k. The numerical values for the critical exponent γ (and also for $(2-\alpha)$ and β) are collected in Figure 4 as a function of k.

The fractal dimension, D, of the percolating cluster can be defined as:

$$s_{perc} \propto L^D \qquad (\text{at} \quad p = p_c) \tag{16}$$

where s_{perc} represents the number of elements which form the spanning cluster. Thus, in Figure 7b s_{perc} at p_c versus L/k is plotted in a log-log scale for different values of k, as indicated. The slopes of these parallel curves give an estimation of the fractal dimension of the percolating cluster. The values obtained are presented as a function of k in Figure 4.

At $p = p_c$, the scaling theory also predicts that

$$n_s(p) \propto s^{-\tau}. \tag{17}$$

Thus, from its definition, it is seen that the slope of $\ln n_s$ versus $\ln s$ gives the exponent τ. In Figure 7c, this relation is plotted for different values of k as indicated. Numerical values of τ are collected in Figure 4 as a function of k. A compilation of the numerical values of the critical exponents obtained here is presented in Table 1.

In summary, it can be concluded that the phase transition involved in the problem considered in the present paper belongs to the same universality class of the random percolation. This conclusion is also valid when either the percolating species is a linear segment or the k-mers can be dropped only on the bonds of the lattice.

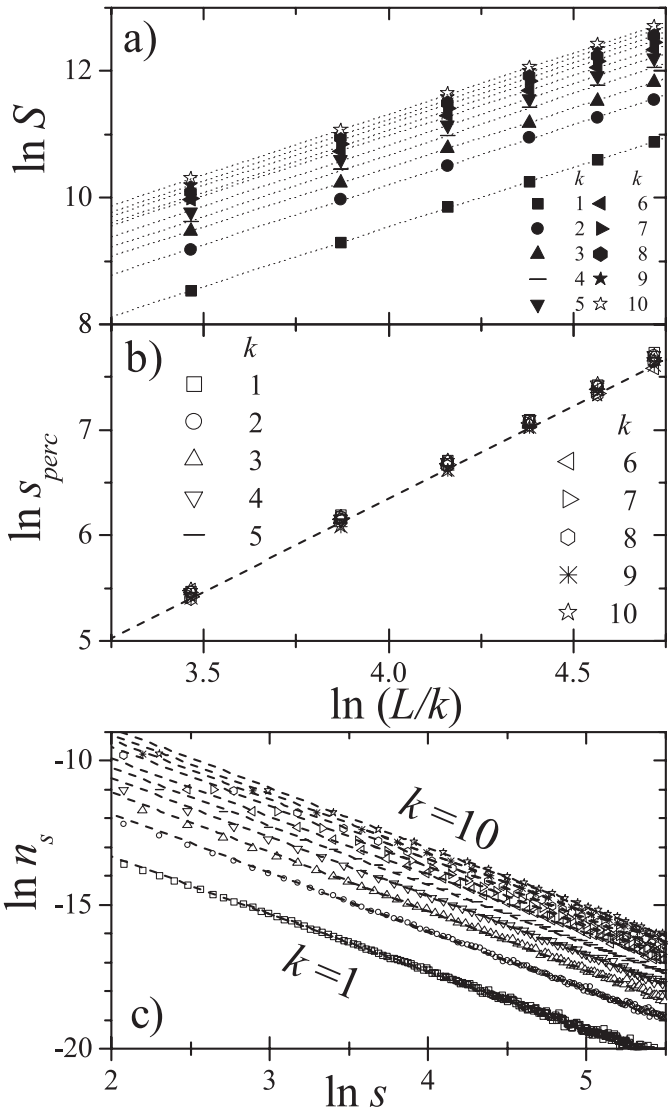

Fig. 7. a) The average cluster size, S (second moment of the n_s distribution) as a function of the rate L/k (log-log scale) for different values of k as indicated. b) $\ln s_{perc}$ at p_c versus $\ln(L/k)$ for different values of k, as indicated. s_{perc} represents the number of elements forming the spanning cluster. c) $\ln n_s$ versus $\ln s$ at p_c for different values of k as in the previous figures. The slopes of these parallel curves give an estimation of the critical exponents γ (a), D (b) and τ (c), respectively. Their numerical values are collected in Figure 4. The fact that all the lines in each graphic are parallel is a clear insight of the universal character of the associated critical exponent.

4 The percolation threshold

In this section we shall focus on the behavior of the percolation threshold as a function of the k-mer size. We shall also examine how that result is modified as the percolating k-mers are simply linear segments as it was considered previously by Leroyer and Pommiers [32,33]. Finally, we shall consider how the percolation threshold changes when k-mers of different sizes are distributed on a bond lattice of square symmetry.

In Figure 8, the percolation threshold for linear segments (open circles) is plotted as a function of k. At the beginning, for small values of k, the curve rapidly decreases. However, it flatten out for larger values of k and finally asymptotically converges towards a definite value as $k \to \infty$. The fact that $p_c(k)$ does not approach zero

Table 1. Compilation of the numerical values of the critical exponents. ν_a (ν_b) denotes the values of the exponent ν as it is evaluated with the methodology of Figure 3a (Fig. 3b).

k	$(2-\alpha)$	γ	τ	D	ν_a	ν_b	β
1	2.598(7)	2.427(2)	2.001(10)	1.889(44)	1.369(36)	1.347(21)	0.131(5)
2	2.588(16)	2.452(13)	2.035(12)	1.854(52)	1.368(24)	1.373(23)	0.121(13)
3	2.571(8)	2.410(29)	2.048(13)	1.879(76)	1.406(26)	1.309(12)	0.123(10)
4	2.603(19)	2.442(20)	2.041(13)	1.845(4)	1.366(26)	1.379(9)	0.139(10)
5	2.600(18)	2.435(9)	2.067(17)	1.840(53)	1.361(12)	1.354(5)	0.147(4)
6	2.581(10)	2.426(25)	2.040(21)	1.922(13)	1.354(9)	1.334(12)	0.154(11)
7	2.632(32)	2.416(41)	2.038(14)	1.845(30)	1.361(7)	1.339(21)	0.140(16)
8	2.607(29)	2.422(17)	2.068(17)	1.836(48)	1.348(5)	1.357(12)	0.147(11)
9	2.602(80)	2.414(12)	2.036(11)	1.904(12)	1.354(12)	1.335(11)	0.175(15)
10	2.574(5)	2.382(55)	2.044(25)	1.893(11)	1.328(20)	1.312(10)	0.189(10)

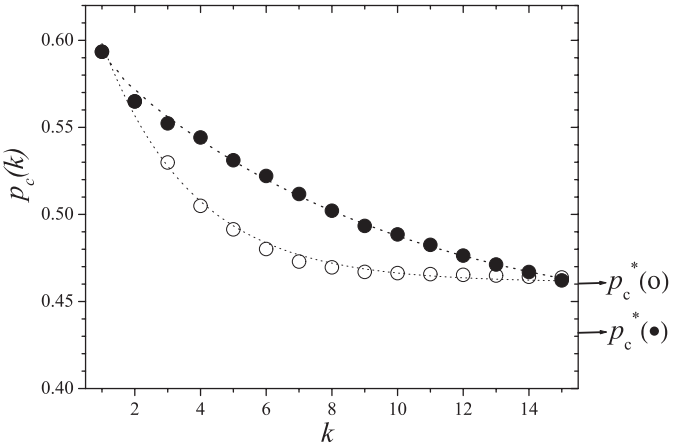

Fig. 8. The percolation threshold as a function of k for linear segments (open circles) and for any form of the k-mer (filled circles). Percolation on sites of a square lattice is considered. The behavior of the fitting curves are described according to equation (18). The error in each measurement is specified but in most of the cases it is smaller that the size of the symbols. The asymptotic limits, p_c^*, [$p_c(k)$ for $k \to \infty$] are shown.

when k goes to infinity is a consequence of the order in which limits are taken since clearly when k is infinity it will always give a percolating cluster. A compilation of the numerical values is also presented in the first column of Table 2. In previous studies of the same problem [32,33] an abrupt increment of $p_c(k)$ is observed for values of $k > 10$. This discrepancy with our results is explained because of finite size effect not considered in references [32,33].

The monotonic behavior of the percolation threshold as a function of the linear segment size can be associated to an exponentially decreasing function according to the following expression:

$$p_c(k) = p_c^* + \Omega \exp\left[-\frac{k}{\kappa}\right] \tag{18}$$

being p_c^*, Ω and κ fitting parameters. p_c^* is the expected value in the limit $k \to \infty$. It is important to note that the curve $p_c(k)$ does not respond to a $1/k$ behavior as it

Table 2. Compilation of the numerical values of the percolation thresholds for linear segments, p_c^{ls} (second column) and for any form of the k-mer, p_c^s (third column) in the site percolation problem. p_c^b (fourth column) gives the corresponding values of the percolation threshold for the bond percolation.

k	p_c^{ls}	p_c^s	p_c^b
1	0.593(2)	0.593(2)	0.5009(2)
2	0.564(2)	0.564(2)	0.4859(2)
3	0.529(2)	0.552(2)	0.4732(2)
4	0.504(2)	0.542(2)	0.4630(2)
5	0.491(2)	0.531(2)	0.4565(2)
6	0.480(2)	0.522(2)	0.4497(2)
7	0.472(2)	0.511(2)	0.4423(2)
8	0.469(2)	0.502(2)	0.4348(2)
9	0.467(2)	0.493(2)	0.4291(2)
10	0.466(2)	0.488(2)	0.4232(2)
11	0.465(2)	0.482(2)	0.4159(2)
12	0.465(2)	0.476(2)	0.4114(2)
13	0.464(2)	0.471(2)	0.4061(2)
14	0.464(2)	0.467(2)	0.4011(2)
15	0.463(2)	0.462(2)	0.3979(2)

was predicted in references [32,33]. In fact, Leroyer and Pommiers [32] mentioned in their contribution that the modelization used (oriented boxed by rigid boxes) "is presumably too simple to explain the slight rise for large k, which may be due to the interpenetrability of these regions and/or to their anisotropy".

The fitting parameters obtained for percolation of linear segments of size k are the following: $p_c^* = 0.461 \pm 0.001$, $\Omega = 0.197 \pm 0.02$ and $\kappa = 2.775 \pm 0.02$.

Once studied the problem of percolating linear segments, we shall discuss the case of percolating k-mers regardless of its form. For this case, in Figure 8, the percolation threshold as a function of k is plotted by using filled circles (see also second column of Tab. 2). The behavior of the curve is qualitatively similar to that discussed above according to equation (18). However, for this case, the

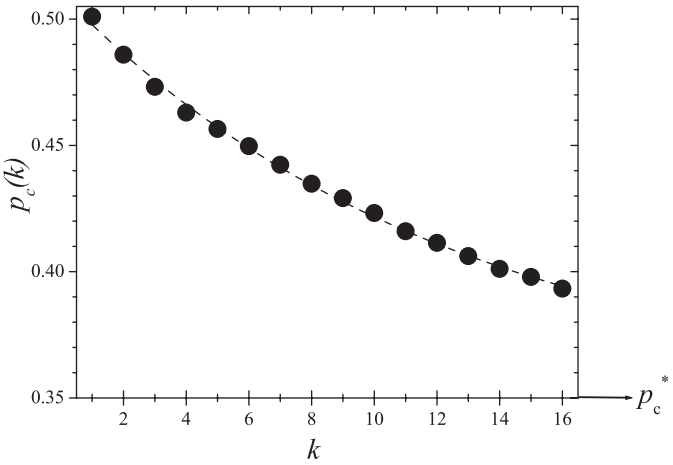

Fig. 9. The percolation threshold as a function of k for percolation on bonds of a square lattice. The line represents the fitting according to equation (18). The error in each measurement is specified but in most of the cases it is smaller that the size of the symbols. The asymptotic limit, p_c^*, ($p_c(k)$ for $k \to \infty$) is shown.

fitting parameters are $p_c^* = 0.431 \pm 0.001$, $\Omega = 8.175 \pm 0.02$ and $\kappa = 8.83 \pm 0.02$. These results show that the fitting parameters depend on the form and structure of the percolating k-mer besides the properties of the lattice where the k-mers are distributed.

In order to give an example of the veracity the last conclusion, we have studied the percolation of k-mers on the bonds of a square lattice. In this case, the behavior of $p_c(k)$ is also reflected by a exponentially decreasing function as in equation (18), see Figure 9 and the third column of Table 2 as well. In this case, the fitting parameters are $p_c^* = 0.349 \pm 0.001$, $\Omega = 0.16 \pm 0.02$ and $\kappa = 12.47 \pm 0.02$. This shows that the coordination number of the lattice also plays an important role for determining the values of the fitting parameters. As it was discussed in Section 3 this problem also belongs to the random percolation universality class.

The dependence of the percolation threshold as a function of k obtained here is consistent with the behavior observed in reference [43] for different two dimensional geometries.

5 Conclusions

In the present paper, the monotonic behavior of the critical concentration has been studied for percolating systems of (a) linear segments of size k; (b) k-mers of different structures and forms deposited on a square lattice (site and bond percolation). It was established that the percolation threshold exhibits a exponentially decreasing function when it is plotted as a function of the k-mer size. The fitting parameters of that function are dependent not only on the form and structure of the k-mers but also on the properties of the lattice where they are deposited (for example, the coordination number).

In order to test the universality of the problem, the phase transition involved on it has been studied by using finite-size scaling theory. In particular, it was established that (a) the scaling functions are dependent with respect to the k-mers size and (b) the problem, in all the studied cases, belongs to the random percolation universality class. The last conclusion is confirmed by determining the numerical values of the critical exponents, α, β, γ, ν, τ and the fractal dimension D of the spanning cluster. In addition, the corresponding curves collapse according to the predictions of the finite size scaling theory.

Finally, the importance of the effect of this particular degree of local correlation, determined by the k-mers, on the percolation threshold is addressed.

This work has been supported by CONICET (Argentina), Fundación Antorchas (Argentina) and by the National Agency for Promotion of Science and Technology (APCyT, Argentina), Proy. PICT98 N° C-03-03232.

References

1. J.M. Hammersley, Proc. Cambridge Phil. Soc. **53**, 642 (1957)
2. D. Stauffer, *Introduction to Percolation Theory* (Taylor & Francis, 1985)
3. *Percolation Structures and Processes*, edited by G. Deutscher, R. Zallen, J. Adler, Ann. Israel Phys. Soc., Vol. 5 (Ayalon Offset Ldt, 1983)
4. M. Sahimi, *Application of the percolation theory* (Taylor & Francis, London, 1992)
5. R. Zallen, *The Physics of Amorphous Solids* (John Willey & Sons, NY, 1983)
6. S. Kirkpatrick, Rev. Mod. Phys. **45**, 574 (1973)
7. J.W. Essam, Rep. Progr. Phys. **43**, 843 (1980)
8. J.-P. Hovi, A. Aharony, Phys. Rev. B **53**, 235 (1996)
9. K. Binder, Rep. Progr. Phys. **60**, 488 (1997)
10. R.H. Fowler, G.S. Rushbrooke, Trans. Faraday Soc. **33** 1272 (1937)
11. P.J. Flory, J. Chem. Phys. **10**, 51 (1942)
12. P.J. Flory, *Principles of polymer chemistry* (Cornell University Press, Ithaca, NY, 1953)
13. A.J. Phares, J. Math. Phys. **25**, 1756 (1984)
14. A.J. Phares, F.J. Wunderlich, J.D. Curley, D.W. Grumbine Jr., J. Phys. A: Math. Gen. **26**, 6847 (1993)
15. P.W. Kasteleyn, Phys. **27**, 1209 (1961)
16. M.E. Fisher, Phys. Rev. **124**, 1664 (1961)
17. A.J. Ramirez-Pastor, J.L. Riccardo, V.D. Pereyra, Surf. Sci. **411**, 294 (1998)
18. J.E. González, A.J. Ramirez-Pastor, V.D. Pereyra, Langmuir **17**, 6974 (2001)
19. F. Romá, A.J. Ramirez-Pastor, J.L. Riccardo, Langmuir, **16**, 9406 (2000); J. Chem. Phys. **114**, 10932 (2001)
20. W. Rżysko, M. Borówko, J. Chem. Phys. **117**, 4526 (2002); Surf. Sci. **520**, 151 (2002)
21. J.W. Evans, Rev. Mod. Phys. **65**, 1281 (1993)
22. V. Privman, J.-S. Wang, P. Nielaba, Phys. Rev. B **43**, 3366 (1991)

23. V.D. Pereyra, E.V. Albano, J. Phys. A **26**, 4175 (1993)
24. E.V. Albano, V.D. Pereyra, J. Chem. Phys. **98**, 10044 (1993)
25. J.W. Evans, D.E. Sanders, Phys. Rev. B **39**, 1587 (1989)
26. A. Bunde, H. Harder, W. Dieterich, Solid State Ionics **18 & 19**, 156 (1986)
27. H. Harder, A. Bunde, W. Dieterich, J. Chem. Phys. **85**, 4123 (1986)
28. H. Holloway, Phys. Rev. B **37**, 874 (1988)
29. M. Nakamura, Phys. Rev. A **36**, 2384 (1987)
30. M. Henkel, F. Seno, Phys. Rev. E **53**, 3662 (1996)
31. E.L. Hinrichsen, J. Feder, T. Jossang, J. Stat. Phys. **44**, 793 (1986)
32. Y. Leroyer, E. Pommiers, Phys. Rev. B **50**, 2795 (1994)
33. B. Bonnier, M. Honterbeyrie, Y. Leroyer, C. Meyers, E. Pommiers, Phys. Rev. B **49**, 305 (1994)
34. Z. Gao, Z.R. Yang, Physica A **255**, 242 (1998)
35. M. Aizenman, Nuclear Phys. B **485**, 551 (1997)
36. J. Cardy, J. Phys A **31**, L105 (1998)
37. L.N. Shchur, S.S. Kosyakov, Int. J. Mod. Phys. C **8**, 473 (1997)
38. L.N. Shchur, *Incipient Spanning Clusters in Square and Cubic Percolation,* in Springer Proceedings in Physics, Vol. 85, edited by D.P. Landau, S.P. Lewis, H.B. Schuettler (Springer Verlag, Heidelberg, Berlin, 2000)
39. F. Yonezawa, S. Sakamoto, M. Hori, Phys. Rev. B **40**, 636 (1989)
40. F. Yonezawa, S. Sakamoto, M. Hori, Phys. Rev. B **40**, 650 (1989)
41. J. Hoshen, R. Kopelman, Phys. Rev. B **14**, 3428 (1976)
42. V. Privman, P.C. Hohenberg, A. Aharony, *Universal Critical-Point Amplitude Relations*, in Phase Transitions and Critical Phenomena, edited by C. Domb, J.L. Lebowitz, Vol. 14, Chap. 1 (Academic, NY, 1991), pp. 1–134 and 364–367.
43. V. Cornette, A.J. Ramirez-Pastor, F. Nieto, Physica A **327**, 71 (2003)